Published in *Materials Science and Engineering A*, 656, 2016, 55-66. Doi: 10.1016/j.msea.2016.01.027

The significance of self-annealing at room temperature in high purity copper processed by high-pressure torsion

Yi Huang[a, *], Shima Sabbaghianrad[b], Abdulla I. Almazrouee [c], Khaled J. Al-Fadhalah[d], Saleh N. Alhajeri[c], Terence G. Langdon[a,b]

[a]*Materials Research Group, Faculty of Engineering and the Environment, University of Southampton, Southampton SO17 1BJ, U.K.*
[b]*Departments of Aerospace & Mechanical Engineering and Materials Science, University of Southern California, Los Angeles, CA 90089-1453, U.S.A.*
[c]*Department of Manufacturing Engineering, College of Technological Studies, P.A.A.E.T., P.O. Box 42325, Shuwaikh 70654, Kuwait*
[d]*Department of Mechanical Engineering, College of Engineering &Petroleum, Kuwait University, P.O. Box 5969, Safat 13060,Kuwait*
*Corresponding author: y.huang@soton.ac.uk (Yi Huang)

Abstract

High purity copper was processed by high-pressure torsion (HPT) at room temperature and then stored at room temperature for periods of up to 6 weeks to investigate the effect of self-annealing. Hardness measurements were recorded both at 48 h after HPT processing and after various storage times. The results show the occurrence of recovery near the edges of the discs after processing through 1/2 and 1 turn and this leads to a significant drop in the measured hardness values which is accompanied by microstructural evidence for abnormal grain growth. Conversely, there was no recovery, and therefore no hardness drops, after processing through 5 and 10 turns. X-ray line profile analysis was used to determine the crystallite sizes and dislocation densities at 1 h after HPT and after storage for different times. The results show a good thermal stability in high purity Cu after processing through more than 1 turn of HPT but care must be exercised in recording hardness measurements when processing through only fractional or very small numbers of turns.

Keywords: copper; grain growth; hardness; high-pressure torsion; self-annealing.

1. Introduction

Equal-channel angular pressing (ECAP) and high-pressure torsion (HPT) are currently the most efficient severe plastic deformation (SPD) techniques for producing high-strength ultrafine-grained (UFG) and nanostructured materials [1-4]. However, the processes are different because ECAP is not continuous whereas in HPT it is possible to achieve a very high strain in a single operation. Furthermore, HPT is advantageous by comparison with ECAP because it produces smaller grains [5,6] and also a higher fraction of grain boundaries having high angles of misorientation [7]. In HPT, a very high compressive pressure is applied to a thin disc and this generates large frictional forces so that the disc may be subjected to torsional deformation without incurring any slippage [8]. Processing by HPT has attracted considerable attention over the last decade because of the potential for achieving a very high shear strain with significant grain refinement and a marked improvement in the mechanical properties. Nevertheless, it is clear that the ability to fabricate nanocrystalline materials for use in practical environments requires not only the development of an exceptionally refined microstructure but also the ability to maintain this microstructure over a significant period of time.

Many reports are now available describing the application of SPD for achieving grain refinement in pure copper using ECAP [9-71], HPT [36,72-113] or a combination of both procedures [36,114,115]. However, it appears that pure copper has a significant disadvantage because of its relatively low thermal stability. There have been several investigations of the thermal stability of copper under various annealing conditions at elevated temperatures after processing by ECAP [27,31] and HPT [72,80,82]. In addition, there is a report of the low temperature annealing of HPT-processed Cu at 373 K for short times up to 60 min but with no significant variations in the measured hardness [109].

An important consideration in the production of UFG materials concerns the potential for self-annealing when holding for long times at room temperature (RT). Thus, experiments on a Cu wire heavily-deformed by drawing showed the occurrence of a significant decrease in strength after RT storage for periods up to 12 months [116]. The long-term RT storage of cryogenically-rolled copper was examined for periods up to 1.5 years and there was direct evidence for grain boundary migration and recovery [117]. The microstructures of copper samples processed by ECAP were examined following RT storage for a period of 8 years and there was evidence for recrystallization [118] and recrystallization was also reported in high purity Cu single crystals processed by ECAP and subjected to RT storage for 2 months [119]. For processing by HPT, there is a report on short term (100 h) RT self-annealing in Cu with a continuous decrease in hardness [108]. In addition to reports on Cu, it is now well established that there are significant drops in the hardness of high purity Ag after processing by ECAP and holding in storage at room temperature for up to 4 months [120,121]. All of these results demonstrate that the hardness values recorded in Cu after HPT, and possibly also in other materials, may depend upon the time that elapses between the processing operation and the measurements of hardness.

A comprehensive review of hardness measurements in metals processed by HPT reveals three different trends [122]. First, most metals, including Cu, show an increasing hardness with increasing strain until attaining a saturation plateau in the process designated hardening without recovery. Second, pure Al shows an increase in hardness followed by a subsequent decrease to a saturation level in the process known as softening with rapid recovery where the recovery occurs because of the high stacking fault energy. Third, some materials show a weakening to a saturation level after HPT processing. Although it is generally recognized that Cu follows the conventional hardening without recovery as in almost all metals, some very recent results suggest that self-annealing may be important.

Thus, in experiments on high purity (99.99+ wt.%) oxygen free high conductivity (OFHC) copper it was reported that the hardness initially increased up to an equivalent strain of ~2, decreased to a strain of ~8 and then increased again to a saturation value at a strain >22 [111]. Furthermore, these unusual results were consistent with earlier data reported for OFHC Cu in experiments conducted at room temperature using repetitive upsetting-extrusion where the material was subjected to repeated upsetting and extrusion [123]. Accordingly, and in order to further investigate the significance of these results, the present investigation was initiated to determine the precise values of the Vickers microhardness in discs processed by HPT and then stored at room temperature for periods of up to a maximum of 6 weeks.

2. Experimental material and procedures

As in the earlier experiments [111], the experiments were conducted using a rod of high purity OFHC copper of 99.99+ wt% purity. The chemical composition is given in Table 1. The rod was initially annealed for 1 h at 673 K and then cut into discs with diameters of 10 mm and thicknesses of ~0.8 mm. The discs were processed by HPT at RT through total numbers of turns, N of 1/2, 1, 5 and 10. The processing was conducted using an applied pressure of 6.0 GPa, the rotation speed was 1 rpm and the processing was conducted under quasi-constrained conditions where there is a small amount of outflow around the edge of the disc between the two anvils [124,125]. Following HPT, discs were stored at RT for periods up to 6 weeks.

For measurements of the microhardness, both the HPT-processed discs and the post-HPT stored discs were carefully ground with SiC papers in order to remove layers of ~0.1 mm thickness from the disc surfaces. The discs were then polished with 9, 6, 3 and 1 μm diamond suspensions and polished to a mirror-like surface using a vibratory polisher with 0.04 μm colloidal silica. The Vickers microhardness, Hv, was measured on the polished surfaces using an FM300 microhardness tester equipped with a Vickers indenter. Each

hardness indentation was performed using a load of 200 gf and a dwell time of 15 s. These measurements were taken at positions along the disc diameters separated by incremental distances of 0.3 mm and with the average hardness at each position estimated from four individual points recorded around the selected position and separated by distances of 0.15 mm. These measurements gave the variations of hardness across each disc together with the associated error bars recorded at the 95% level.

The grain structures in the HPT-processed and the post-HPT stored discs were examined near the centre of each disc and at positions ~1.5 and ~3.5 mm from the disc centres, respectively. Microstructural examinations were conducted with electron backscattered diffraction (EBSD) using an analytical field emission scanning electron microscope (SEM) JEOL JSM-7001F at an operating voltage of 15 kV. The SEM was equipped with imaging detectors and used a TSL orientation imaging system and OIM™ software for data collection.

The microstructures of the HPT-processed samples were evaluated using a Bruker D2 Phaser X-ray diffractometer equipped with a Cu target using Cu Kα (wavelength λ = 0.15406 nm) radiation and a Ni monochromator with a 1D LYNXEYE detector. It is important to note that the whole disc surface was analysed by X-ray diffraction (XRD) and θ - 2θ scans were conducted from 2θ = 25° to 100° with scan steps of 0.02° to record the XRD patterns. The crystallite size, the lattice parameter and the microstrain $<\varepsilon^2>^{1/2}$ were calculated based on the Rietveld method [126] using Maud software for profile fitting. The XRD patterns were recorded for the annealed Cu and after HPT processing through 1/2, 1, 5 and 10 turns and subsequent RT storage for different periods of time.

The microhardness measurements, microstructure characterisation and XRD analysis were performed on the Cu disc samples approximately 48 h after HPT processing and after post-HPT RT storage for periods of 1, 2, 3 and 4 weeks.

3. Experimental results

3.1 Hardness and microstructure at 48 h after HPT processing

In the initial annealed condition, the high purity Cu had an average grain size of ~85 μm and an average Vickers microhardness of Hv ≈ 41.

The evolution in hardness with increasing numbers of HPT turns is shown in Fig. 1 where the experimental points were recorded across the discs at 48 h after the HPT processing and after 1/2 to 10 turns. Inspection shows that the results generally appear consistent with conventional face-centred cubic (fcc) metals. After 1/2 and 1 turn the hardness values are similar to 5 and 10 turns around the peripheries of the discs but in the central region, within ~1.5 mm of the central point, the values are lower than at the edge. After 5 and 10 turns the hardness values are reasonably homogeneous across the disc diameters and the values have reached an essentially stable condition. In practice, however, the values after 5 and 10 turns are slightly lower than the plateau hardness values recorded at the edge after 1/2 and 1 turn and this suggests the onset of some limited structural recovery after the higher numbers of turns. Thus, the slightly higher values at the mid-radius positions after 1/2 turn are similar to but smaller than the higher hardness values reported at these positions after processing for fractional numbers of a turn in high purity Al [127].

Figure 2 shows the microstructural development after 1/2 and 10 turns in different positions on the discs at 48 h after HPT processing; the colours in Fig. 2 denote different grain misorientations as depicted in the unit triangle, low-angle grain boundaries (LAGBs) of 2°-15° are shown in yellow and high-angle grain boundaries (HAGBs) of >15° are marked in black. The upper images in Fig. 2 illustrate the microstructures after 1/2 turn at the disc centre, at 1.5 mm from the centre and at 3.5 mm from the centre, respectively. Thus, after 1/2 turn there is a very significant grain refinement at 3.5 mm from the centre of the disc with a

measured grain size of ~0.5 μm, the disc centre retains a coarse grain structure containing subgrain networks within the coarse grains and at 1.5 mm from the centre the situation is intermediate with grains that are larger than at the edge but smaller than at the centre. As torsional straining is continued to 10 turns in the two lower images in Fig. 2, the microstructures in the centre and the edge become reasonably uniform with an average grain size in both areas of ~0.5 μm. It is readily apparent from Figs 1 and 2 that there is a microstructure gradient, and therefore a strength gradient, from the centres to the edges after 1/2 and 1 turn.

3.2 Hardness development during post-HPT RT storage

In order to obtain a comprehensive understanding of the hardness and microstructure development during post-HPT RT storage, HPT-processed Cu discs were carefully examined following a rigid time schedule after storage for 1, 2, 3, 4 and 6 weeks. The hardness measurements recorded on these samples are shown in Fig. 3 for (a) 1/2, (b) 1, (c) 5 and (d) 10 turns: for each condition, separate hardness values are recorded after time periods of 48 h and then 1, 2, 3, 4 and 6 weeks. For 1/2 turn, as shown in Fig. 3 (a), the hardness values are lower in the centre, increase towards the edges up to ~1.5 mm from the centre and then within this region the results remain unchanged during the storage period from 48 h to 6 weeks. However, from the position of ~1.5 mm to the edge of the disc the hardness changes significantly from week 1 to week 6. Thus, at week 1 there is a slight hardness drop, at week 2 this drop becomes more significant, it develops further at week 3 and at week 4 the hardness attains a reasonably stable state of relatively low hardness which remains unchanged without any additional decrease at week 6.

These results may be summarized by noting that, for the 1/2 turn sample in the area beyond ~1.5 mm from the disc centre, there is a significant drop in the local hardness from the disc half-radius to the edge at 6 weeks of post-HPT RT storage such that the hardness

changes from an initial value of Hv ≈ 41 before HPT, increases to Hv ≈ 140 Hv within 48 h of HPT and then drops to Hv ≈ 80 after both 4 and 6 weeks of storage. In Fig. 3(b) the measurements are plotted after 1 turn where there is a hardness drop from a position of ~1 mm from the disc centre to the half-radius position but there is no change in hardness either at the edge of the disc or in the central area. Careful inspection of Fig. 3(b) shows no obvious local hardness drop at 1 week, a slight local hardness drop at 2 weeks and then significant drops at 3 to 6 weeks. The maximum local hardness drop is from Hv ≈ 140 at 48 h to Hv ≈ 80 at 6 weeks, thereby demonstrating a reduction in hardness of ~43%. At even larger numbers of turns, as with 5 and 10 turns in Fig. 3(c) and (d), there is essentially a constant hardness throughout the period from 48 h to 6 weeks.

These results show that the measured hardness values remain constant and independent of the storage times when the discs are processed through 5 or 10 turns whereas after 1/2 or 1 turn there are local hardness drops during post-HPT RT storage but a low and stable hardness is reached after 4 or more weeks of storage. Therefore, the results demonstrate the importance of conducting HPT processing of any material to include hardness measurements after at least some fractional numbers of turns.

3.3 Microstructure development in 1/2 turn disc during post-HPT RT storage

Since samples processed through 5 and 10 turns show constant hardness during RT storage from 48 h to week 6 in Fig. 3, it is important to concentrate on discs showing local hardness drops during post-HPT RT storage. Accordingly, attention was devoted primarily to the evolution of microstructure in post-HPT storage after processing through 1/2 turn.

Figure 4 illustrates the microstructural development in 1/2 turn samples after 1, 2, 3 and 4 weeks of RT storage, where the left, centre and right columns show microstructures in the disc centre and at 1.5 and 3.5 mm from the centre, respectively: for ease of reference, all images are shown at the same magnification. In week 1, the microstructures are similar to

those after 48 h as shown in Fig. 2 (a)–(c) with coarser grains in the centre, very refined grains at the edge and an intermediate grain size at the 1.5 mm position. With increasing storage time to 2, 3 and 4 weeks, there are no significant microstructural changes in the centre or at 1.5 mm from the centre whereas at the edge it is evident that a few grains grow to a large size while most of the grains remain refined and similar to those observed after storage for 48 h. These larger grains continue to grow and ultimately occupy almost two-thirds of the observation area in a process which may be classified as abnormal grain growth. The occurrence of this abnormal growth at the disc edge area, at 3.5 mm from the centre, correlates well with the local drop in hardness as shown in Fig. 3(a).

The fractional numbers of grain boundaries having different misorientation angles at 3.5 mm from the disc centre are displayed in Fig. 5 for incremental angular intervals of 5° after periods of RT storage from 48 h to 4 weeks after HPT. Generally, it is apparent that the fraction of HAGBs increases with increasing storage time at RT and this is especially evident for misorientation angles in the range of 55-60° where there are large numbers of ∑3 twin boundaries. In order to more effectively illustrate this evolution, Fig. 6 shows the number fractions of the sums of LAGBs, ∑3 boundaries and HAGBs plotted without including the ∑3 boundaries after RT storage through different times. Thus the number fractions of LAGBs show a slight decrease with increasing storage time whereas the number fractions of ∑3 boundaries is relatively stable between 48 h and 2 weeks but then increases in weeks 3 and 4 to reach a maximum fraction of ~14.3% after storage for 4 weeks. It is well established that in fcc metals having low to medium stacking fault energies the most important Coincident Site Lattice (CSL) boundary is ∑3 which is dominated by the formation of annealing twins [128]. Based on the increase of ∑3 boundaries with increasing storage time in Fig. 6 and the drop in hardness by ~43% from ~140 Hv to ~80 Hv in the 1/2 and 1 turn

samples as shown in Fig. 3(a) and (b), it is reasonable to conclude that recrystallization occurs in high purity Cu during RT storage.

3.4 Microstructural results from X-ray line profile analysis

Using X-ray line profile analysis for materials subjected to severe plastic deformation, the dislocation density, ρ, may be calculated using the relationship [129-131]

$$\rho = \frac{2\sqrt{3}\left\langle \varepsilon^2 \right\rangle^{\frac{1}{2}}}{D_c \times b} \quad (1)$$

where b is the Burgers vector equal to $a/\sqrt{2}$ for fcc metals where *a* is the lattice parameter, D_c is the crystallite size and $<\varepsilon^2>^{1/2}$ is the microstrain in XRD.

Figure 7 shows the calculated microstrains and dislocation densities plotted as a function of the numbers of turns in the HPT-processed Cu after RT storage for (a) 1h, (b) 1 week and (c) 4 weeks. It is readily apparent that immediately after HPT processing, as denoted by storage for 1 h in Fig. 7(a), the microstrain increases with numbers of HPT rotations from 1/2 to 1 turn but thereafter it decreases as the number of HPT rotations increases to 5 and then 10 turns. Furthermore, the calculated dislocation densities are consistent with the microstrains with an initial increase from ~5.7 × 10^{13} m^{-2} for 1/2 turn to ~6.0 × 10^{13} m^{-2} for 1 turn and then a drop to ~2.4 × 10^{13} m^{-2} after 5 turns and a further drop to ~1.5 × 10^{13} m^{-2} after 10 turns. The decrease in microstrian and dislocation density from 5 to 10 turns is consistent with the observation in Fig. 1 that the overall hardness values after 5 and 10 turns are slightly lower than the hardness value at the disc edge after 1/2 and 1 turn. The drop in dislocation density from 5 to 10 turns indicates the occurrence of some recovery in the 5 and 10 turns samples within 1 h of the HPT processing.

As shown in Fig. 7(b), the microstrain and dislocation density after RT storage for 1 week show a similar trend to the data after 1h after HPT processing although the dislocation

densities in the 1/2 and 1 turn samples are now lower. This matches the hardness results in Fig. 3 where there is a slight hardness drop in the 1/2 and 1 turn samples afters 1 week of storage. After 4 weeks of RT storage the microstrains and dislocation densities in Fig. 7(c) show a different trend where the 1/2 turn sample gives a higher microstrain and dislocation density than after 1 turn and thereafter there is a relatively small drop in microstrian and dislocation density at 5 and 10 turns.

The crystallite sizes estimated from an XRD line broadening analysis are shown in Fig. 8 after (a) 1/2 turn and (b) 10 turns for samples stored at RT for up to 4 weeks. In Fig. 8(a) there is a minor but consistent increase in the crystallite size during storage from 1 h to 4 weeks which is consistent with the microstructures in Fig. 4 where there is abnormal grain growth during RT storage of the 1/2 turn sample. For the 10 turn sample shown in Fig. 8 (b), the crystallite size remains essentially constant during RT storage from 48 h to 4 weeks which is consistent with the microhardness data in Fig. 3(d).

4. Discussion

4.1 General observations on the effect of self-annealing in high purity Cu processed by HPT

Although there have been many reports documenting the microstructural evolution and microhardness in high purity Cu processed by HPT, a careful review shows there was only a single attempt to evaluate the occurrence of self-annealing on the measured values of microhardness recorded after HPT processing [132]. In the latter investigation, Cu of 99.99% and 99.99999% purity was processed by HPT either at RT or at a cryogenic temperature of 100 K and then hardness measurements were recorded after storage at RT for various periods of time. The results showed that samples processed by HPT at 100 K exhibited a very significant self-annealing after storage for a few hours and this self-annealing effect was greater in the ultra-high purity 99.99999% Cu than in the 99.99% Cu. Furthermore, the self-annealing effect was relatively minor in the two grades of Cu processed by HPT at RT such

that there was a drop of only ~22 Hv in the 99.99% Cu after processing at RT and then storing at RT for 4.3 years [132].

The present investigation used Cu of 99.99% purity and processed by HPT at RT. The results are consistent with this earlier report except that the present data demonstrate conclusively that self-annealing has a major effect at the onset of HPT processing when samples are processed through 1/2 or 1 turn. Conversely, it is also apparent from Fig. 3(c) and (d) that self-annealing is not significant in samples processed through 5 or more turns. These results show, therefore, that exceptional care is required when processing high purity Cu samples through only fractional numbers of HPT turns since, as is readily apparent from Fig. 3(a), an exceptional drop in hardness by up to ~60 Hv may be anticipated after a wait of several weeks when processing by HPT through up to 1 turn. It is apparent that these drops in hardness during RT storage are not generally recognized in the many earlier reports of the HPT processing of high purity Cu.

4.2 The occurrence of dynamic recovery during HPT processing

In order to more fully understand the hardness measurements shown in Fig. 1, wherein the hardness values after 5 and 10 turns are lower at the disc edge than after 1/2 and 1 turn, it is necessary to examine the overall significance of hardness measurements in HPT. It is well established that the equivalent von Mises strain, ε, may be estimated in HPT using the relationship [133-135]

$$\varepsilon = \frac{2N\pi r}{h\sqrt{3}} \qquad (2)$$

where r and h are the radius and height (or thickness) of the disc, respectively.

In practice, the variation of hardness with equivalent strain is dependent upon the nature of recovery in the material [122,136,137]. It was shown in very early experiments that, although the individual hardness measurements in HPT tend to be scattered in a plot of the type shown in Fig. 1, it is possible to correlate the data by plotting the individual values of Hv

against the equivalent strain as calculated from eq. (2) [138]. In addition, this type of plot also provides a direct measure of the saturation hardness. Accordingly, the values of the Vickers microhardness were plotted against the equivalent strain as shown in Fig. 9 using the individual datum points from Fig. 1 where these hardness values were obtained by averaging the two sets of measurements recorded on either side and equidistant from the centres of the discs.

Inspection of Fig. 9 shows two significant trends. First, pure Cu displays a curve that initially increases rapidly, levels off above an equivalent strain of ~20 and then remains essentially constant at a level of Hv ≈ 130 Hv at equivalent strains above ~50. This result is consistent with other reports of saturation hardness values in the HPT processing of pure Cu of ~130 [89], ~150 [111] and ~142 [112]. Second, as shown in Fig. 9, a higher hardness of ~140 Hv is recorded in the very early stages of HPT processing, at equivalent strains <20, where this is similar to some other results reported in the earliest stages of processing of Cu [90,111,112]. It appears initially that the behaviour in Fig. 9 may be similar to the results reported for high purity Al where there is softening with rapid recovery [139]. However, this early softening is different from the softening in Al because it is well known, both from very early experiments in HPT processing [140,141] and from more recent investigations [98,112], that dynamic recrystallization is important in pure Cu.

The crystallite sizes calculated from an X-ray line profile analysis demonstrate that, as shown in Fig. 8, the size is larger in the 10 turns sample (~160 nm) than in the 1/2 turn sample (~120 nm) at 1 h after HPT processing. It is readily apparent from Fig. 2 that, after storage at RT for 48 h, the 10 turns sample has a uniform grain structures across the disc with and average grain size of ~0.5 μm whereas after 1/2 turn there is a non-uniform grain structure from the centre to the edge with coarse grains in the centre and a grain size of ~0.5 μm at the edge. As noted earlier, the whole disc surface was monitored in the XRD analysis

and therefore these data should include contributions from both the disc centre and the edge area. Since there is a grain structure gradient in the 1/2 turn sample and a uniform grain structure in the 10 turns sample, it is reasonable to anticipate the 1/2 turn sample may exhibit a crystallite size that is larger than in the 10 turns sample. The reason this anticipated trend is not followed lies in the onset of easy recovery in the samples processed through large numbers of HPT turns. Furthermore, the drop in the density of dislocations from 5 to 10 turns within 1 h after HPT processing, as shown in Fig. 7(b), suggests also the occurrence of recovery during processing of the 5 and 10 turns samples.

4.3 The nature of self-annealing in Cu following long-term RT storage

The results from this investigation show the occurrence of a very significant self-annealing effect in high purity Cu after 1/2 turn whereas self-annealing is less important after 1 turn and the effect is absent after 5 and 10 turns. It is evident from Fig. 4 that the self-annealing is associated with the abnormal grain growth that occurs at ~3.5 mm from the disc centre and leads to an array of very large grains mixed with many ultrafine-grains. A similar report of abnormal grain growth and a mix of highly refined and very large grains was reported earlier for high purity Al processed by ECAP through 12 passes [142].

It appears from Fig. 7 that this abnormal growth of grains is specifically associated with a high dislocation density and, from Fig. 6, a reasonable fraction of LAGBs. Accordingly, it is concluded that the self-annealing effect arises from delayed recovery which requires dislocation annihilation through the climb of edge dislocations and/or the cross-slip of screw dislocations.

For climb, the recovery will be aided by the presence of an excess concentration of athermally-produced vacancies that are introduced by the HPT processing but generally are only present in high concentrations at temperatures close to the melting point [143,144]. It was reported that HPT-deformed Cu contains a high density of dislocations and also small

vacancy clusters which arise from the agglomeration of deformation-induced vacancies [93]. Furthermore, recent research using dilatometry measurements demonstrated the annealing out of defects associated with the release of free volume upon linear heating of HPT-deformed Cu [103]. Three stage (A,B,C) annealing kinetics were reported and, during annealing at 300-400 K in stage A, there was an annealing out of crystal lattice defects as well as a relaxation of the grain boundaries [103]. These observations are consistent with the presence in SPD-processed materials of arrays of non-equilibrium grain boundaries containing excess grain boundary energies, long-range elastic stresses and enhanced free volumes [145].

It is well known that the probability of cross-slip is associated with the degree of dislocation dissociation and copper has an intermediate stacking fault energy so that there is a reasonable level of dissociation. In practice, cross-slip occurs through thermal fluctuations in the crystalline lattice and it was shown earlier by calculation that, assuming the cross-slip energy is equal to the constriction energy, the anticipated waiting time for cross-slip in Cu is of a reasonable magnitude so that the occurrence of easy recovery can occur in these UFG structures [121].

All of these results and calculations support the conclusion that recovery occurs easily in high purity Cu after processing by HPT through fractional numbers of turns, thereby producing grain growth and a consequent drop in the measured hardness values as recorded in Fig. 3(a) and (b).

5. Summary and conclusions

1. Experiments were conducted on a high purity Cu to investigate the effect of self-annealing during storage at room temperature after processing by high-pressure torsion.

2. The results show self-annealing is important when discs of Cu are processed through 1/2 or 1 turn. At these low strains, there is a very significant drop in the measured

hardness values near the edges of the discs after storage at room temperature for 2 to 6 weeks. There are no drops in hardness during similar storage of discs processed through 5 or 10 turns.

3. The crystallite sizes and dislocation densities were recorded using X-ray line profile analysis and the microstructures were examined at selected positions and after different storage times. The microstructures show that self-annealing after small numbers of turns is associated with abnormal grain growth that occurs near the edges of the discs and leads to arrays of large grains mixed with ultrafine grains.

4. It is concluded that care is needed in recording hardness measurements in Cu in the early stages of HPT processing because of the possibility of abnormal grain growth and significant reductions in hardness at positions near the edges of the discs.

Acknowledgements

This work was supported in part by the Kuwait University General Facility under Grant No. GE 01/0, in part by the National Science Foundation of the United States under Grant No. DMR-1160966 and in part by the European Research Council under ERC Grant Agreement No. 267464-SPDMETALS.

References

[1] R.Z. Valiev, R.K. Islamgaliev, I.V. Alexandrov, Bulk nanostructured materials from severe plastic deformation, Prog. Mater. Sci. 45 (2000) 103-189.

[2] R.Z. Valiev, T.G. Langdon, Principles of equal-channel angular pressing as a processing tool for grain refinement, Prog. Mater. Sci. 51(2006) 881-981.

[3] A.P. Zhilyaev, T.G. Langdon, Using high-pressure torsion for metal processing: Fundamentals and applications, Prog. Mater. Sci. 53 (2008) 893-979.

[4] T.G. Langdon, Twenty-five years of ultrafine-grained materials: Achieving exceptional properties through grain refinement, Acta Mater. 61 (2013) 7035-7059.

[5] A.P. Zhilyaev, B.-K. Kim, G.V. Nurislamova, M.D. Baró, J.A. Szpunar, T.G. Langdon, Orientation imaging microscopy of ultrafine-grained nickel, Scripta Mater. 46 (2002) 575-580.

[6] A.P. Zhilyaev, G.V. Nurislamova, B.-K. Kim, M.D. Baró, J.A. Szpunar, T.G. Langdon, Experimental parameters influencing grain refinement and microstructural evolution during high-pressure torsion, Acta Mater. 51 (2003) 753-765.

[7] J. Wongsa-Ngam, M. Kawasaki, T.G. Langdon, A comparison of microstructures and mechanical properties in a Cu-Zr alloy processed using different SPD techniques, J. Mater. Sci. 48 (2013) 4653-4660.

[8] K. Edalati, Z. Horita, T.G. Langdon, The significance of slippage in processing by high-pressure torsion, Scripta Mater. 60 (2009) 9-12.

[9] S. Komura, Z. Horita, M. Nemoto, T.G.Langdon, Influence of stacking fault energy on microstructural development in equal-channel angular pressing, J. Mater. Res. 14 (1999) 4044–4050.

[10] W.H. Huang, L. Chang, P.W. Kao, C.P. Chang, Effect of die angle on the deformation texture of copper processed by equal channel angular extrusion, Mater. Sci. Eng. A 307 (2001) 113–118.

[11] H.W. Höppel, Z.M. Zhou, H. Mughrabi, R.Z. Valiev, Microstructural study of the parameters governing coarsening and cyclic softening in fatigued ultrafine-grained copper, Phil. Mag. A 82 (2002) 1781-1794.

[12] S.D. Wu, Z.G. Wang, C.B. Jiang, G.Y. Li, I.V. Alexandrov, R.Z. Valiev, The formation of PSB-like shear bands in cyclically deformed ultrafine grained copper processed by ECAP, Scripta Mater. 48 (2003) 1605-1609.

[13] S.C. Baik, R.J. Hellmig, Y. Estrin, H.S. Kim, Modeling of deformation behavior of copper under equal channel angular pressing, Z. Metallk. 94 (2003) 754-760.

[14] S.C. Baik, Y. Estrin, R.J. Hellmig, H.T. Jeong, H.G. Brokmeier, H.S. Kim, Modeling of texture evolution in copper under equal channel angular pressing, Z. Metallk. 94 (2003) 1189-1198.

[15] J. Kuśnierz, J. Bogucka, Effect of ECAP processing on the properties of cold rolled copper Arch. Metall. Mater. 48 (2003) 173-182.

[16] H. Miyamoto, U. Erb, T. Koyama, T. Mimaki, A. Vinogradov, S. Hashimoto, Microstructure and texture development of copper single crystals deformed by equal-channel angular pressing, Phil. Mag. Lett. 84 (2004) 235–243.

[17] L. Tóth, R. Arruffat Massion, L. Germain, S.C. Baik, S. Suwas, Analysis of texture evolution in equal channel angular extrusion of copper using a new flow field, Acta Mater. 52 (2004) 1885-1898.

[18] F.H. Dalla Torre, R. Lapovok, J. Sandlin, P.F. Thomson, C.H.J. Davies, E.V. Pereloma, Microstructures and properties of copper processed by equal channel angular extrusion for 1–16 passes, Acta Mater. 52 (2004) 4819–4832.

[19] J. Gubicza, N.H. Nam, L. Balogh, R.J. Hellmig, V.V. Stolyarov, Y. Estrin, T. Ungár, Microstructure of severely deformed metals determined by X-ray peak profile analysis, J. Alloys Compds 378 (2004) 248-252.

[20] J. Gubicza, L. Balogh, R.J. Hellmig, Y. Estrin, T. Ungár, Dislocation structure and crystallite size in severely deformed copper by X-ray peak profile analysis, Mater. Sci. Eng. A400-401 (2005) 334-338.

[21] E. Schafler, G. Steiner, E. Korznikova, M. Kerber, M.J. Zehetbauer, Lattice defect investigation of ECAP-Cu by means of X-ray line profile analysis, calorimetry and electrical resistometry, Mater. Sci. Eng. A410-411 (2005) 169-173.

[22] A. Mishra, V. Richard, F. Grégori, R.J. Asaro, M.A. Meyers, Microstructural evolution in copper processed by severe plastic deformation, Mater. Sci. Eng. A410-411 (2005) 290-298.

[23] L. Kunz, P. Lukáš, M. Svoboda, Fatigue strength, microstructural stability and strain localization in ultrafine-grained copper, Mater. Sci. Eng. A424 (2006) 97-104.

[24] M. Furukawa, Y. Fukuda, K. Oh-ishi, Z. Horita and T.G. Langdon, An investigation of deformation in copper single crystals using equal-channel angular pressing, Mater. Sci. Forum 503–504 (2006) 113–118.

[25] A. Mishra, B.K. Kad, F. Gregori, M.A. Meyers, Microstructural evolution in copper subjected to severe plastic deformation: Experiments and analysis, Acta Mater. 55 (2007) 13-28.

[26] W. Skrotzki, N. Scheerbaum, C.-G. Oertel, R. Arruffat-Massion, S. Suwas, L.S. Tóth, Microstructure and texture gradient in copper deformed by equal channel angular pressing, Acta Mater. 55 (2007) 2013-2024.

[27] X. Molodova, G. Gottstein, M. Winning, R.J. Hellmig, Thermal stability of ECAP processed pure copper, Mater. Sci. Eng. A460-461 (2007) 204-213.

[28] Y. Fukuda, K. Oh-ishi, M. Furukawa, Z, Horita, T.G. Langdon, Influence of crystal orientation on the processing of copper single crystals by ECAP, J. Mater. Sci. 42 (2007) 1501-1511.

[29] M. Goto, S.Z. Han, S.S. Kim, N. Kawagoishi, C.Y. Lim, Significance of non-equilibrium grain boundaries in surface damage formation of ultrafine-grained copper in high-cycle fatigue, Scripta Mater. 57 (2007) 293-296.

[30] S.Z. Han, M. Goto, C. Lim, C.J. Kim, S. Kim, Fatigue behavior of nano-grained copper prepared by ECAP, J. Alloys Compd. 434-435 (2007) 304-306.

[31] X. Molodova, A. Khorashadizadeh, G. Gottstein, M. Winning, R.J. Hellmig, Thermal stability of ECAP processed pure Cu and CuZr, Intl. J. Mater. Res. 98 (2007) 269-275.

[32] L. Kommel, I. Hussainova, O. Volobueva, Microstructure and properties development of copper during severe plastic deformation, Mater. Des. 28 (2007) 2121-2128.

[33] M. Greger, R. Kocich, L. Čížek, Grain refining of Cu and Ni-Ti shape memory alloys by ECAP process, J. Achiev. Mater. Manuf. Eng. 20 (2007) 247-250.

[34] N. Kobelev, E. Kolyvanov, Y. Estrin, Temperature dependence of sound attenuation and shear modulus of ultra fine grained copper produced by equal channel angular pressing, Acta Mater. 56 (2008) 1473-1481.

[35] C. Xu, Q. Wang, M. Zheng, J. Li, M. Huang, Q. Jia, J. Zhu, L. Kunz, M. Buksa, Fatigue behavior and damage characteristic of ultra-fine grain low-purity copper processed by equal-channel angular pressing (ECAP), Mater. Sci. Eng. A475 (2008) 249-256.

[36] N. Lugo, N. Llorca, J.M. Cabrera and Z. Horita, Microstructures and mechanical properties of pure copper deformed severely by equal-channel angular pressing and high pressure torsion, Mater. Sci. Eng. A 477 (2008) 366-371.

[37] W.Q. Cao, C.F. Gu, E.V. Pereloma, C.H.J. Davies, Stored energy, vacancies and thermal stability of ultra-fine grained copper, Mater. Sci. Eng. A492 (2008) 74-79.

[38] Y. Zhang, J.T. Wang, C. Cheng, J. Liu, Stored energy and recrystallization temperature in high purity copper after equal channel angular pressing, J. Mater. Sci. 43 (2008) 7326-7330.

[39] R.J. Hellmig, M. Janeček, B. Hadzima, O.V. Gendelman, M. Shapiro, X. Molodova, A. Springer, Y. Estrin, A portrait of copper processed by equal channel angular pressing, Mater. Trans. 49 (2008) 31-37.

[40] H. Miyamoto, K. Harada, T. Mimaki, A. Vinogradov, S. Hashimoto, Corrosion of ultra-fine grained copper fabricated by equal-channel angular pressing, Corros. Sci. 50 (2008) 1215-1220.

[41] W. Blum, Y.J. Li, K. Durst, Stability of ultrafine-grained Cu to subgrain coarsening and recrystallization in annealing and deformation at elevated temperatures, Acta Mater. 57 (2009) 5207-5217.

[42] X. Ma, R. Lapovok, C. Gu, A. Molotnikov, Y. Estrin, E.V. Pereloma, C.H.J. Davies, P.D. Hodgson, Deep drawing behaviour of ultrafine grained copper: modelling and experiment, J. Mater. Sci. 44 (2009) 3807-3812.

[43] N. Lugo, N. Llorca, J.J. Suñol, J.M. Cabrera, Thermal stability of ultrafine grains size of pure copper obtained by equal-channel angular pressing, J. Mater. Sci. 45 (2010) 2264-2273.

[44] A. Zi, Pure copper processed by extrusion preceded equal channel angular pressing, Mater. Character. 61 (2010) 141-144.

[45] X.X. Xu, F.L. Nie, J.X. Zhang, W. Zheng, Y.F. Zheng, C. Hu, G. Yang, Corrosion and ion release behavior of ultra-fine grained bulk pure copper fabricated by ECAP in Hanks solution as potential biomaterial for contraception, Mater. Lett. 64 (2010) 524-527.

[46] F. Salimyanfard, M.R. Toroghinejad, F. Ashrafizadeh, M. Jafari, EBSD analysis of nano-structured copper processed by ECAP, Mater. Sci. Eng. A528 (2011) 5348-5355.

[47] W. Blum, Y.J. Li, Y. Zhang, J.T. Wang, Deformation resistance in the transition from coarse-grained to ultrafine-grained Cu by severe plastic deformation up to 24 passes of ECAP, Mater. Sci. Eng. A528 (2011) 8621-8627.

[48] C.F. Gu, L.S. Tóth, C.H.J. Davies, Effect of strain reversal on texture and grain refinement in route C equal channel angular pressed copper, Scripta Mater. 65 (2011) 167-170.

[49] G.Y. Deng, C. Lu, L.H. Su, X.H. Liu, A.K. Tieu, Modeling texture evolution during ECAP of copper single crystal by crystal plasticity FEM, Mater. Sci. Eng. A534 (2012) 68-74.

[50] Q.W. Jiang, X.W. Li, Effect of pre-annealing treatment on the compressive deformation and damage behavior of ultrafine-grained copper, Mater. Sci. Eng. A546 (2012) 59-67.

[51] N.D. Stepanov, A.V. Kuznetsov, G.A. Salishchev, G.I. Raab, R.Z. Valiev, Effect of cold rolling on microstructure and mechanical properties of copper subjected to ECAP with various numbers of passes, Mater. Sci. Eng. A554 (2012) 105-115.

[52] C.X. Huang, W. Hu, G. Yang, Z.F. Zhang, S.D. Wu, Q.Y. Wang, G. Gottstein, The effect of stacking fault energy on equilibrium grain size and tensile properties of nanostructured copper and copper–aluminum alloys processed by equal channel angular pressing, Mater. Sci. Eng. A556 (2012) 638-647.

[53] Y.C. Dong, Y. Zhang, I.V. Alexandrov, J.T. Wang, Effect of high strain rate processing on strength and ductility of ultrafine-grained cu processed by equal channel angular pressing, Rev. Adv. Mater. Sci. 31 (2012) 116-122.

[54] R.H. Li, Z.J. Zhang, P. Zhang, Z.F. Zhang, Improved fatigue properties of ultrafine-grained copper under cyclic torsion loading, Acta Mater. 61 (2013) 5857-5868.

[55] O.F. Higuera-Cobos, J.M. Cabrera, Mechanical, microstructural and electrical evolution of commercially pure copper processed by equal channel angular extrusion, Mater. Sci. Eng. A571 (2013) 103-114.

[56] S.R. Bahadori, K. Dehghani, F. Bakhshandeh, Microstructure, texture and mechanical properties of pure copper processed by ECAP and subsequent cold rolling, Mater. Sci. Eng.A583 (2013) 36-42.

[57] S.R. Bahadori, K. Dehghani, F. Bakhshandeh, Microstructural homogenization of ECAPed copper through post-rolling, Mater. Sci. Eng. A588 (2013) 260-264.

[58] J. Bach, J.P. Liebig, H.W. Höppel, W. Blum, Influence of grain boundaries on the deformation resistance: insights from an investigation of deformation kinetics and microstructure of copper after predeformation by ECAP, Phil. Mag. 93 (2013) 4331-4354.

[59] T. Ishibashi, Y. Tomota, S. Sugaya, H. Toyokawa, T. Hirade, Z. Horita, H. Suzuki, Bulky averaged microscopic information for ECAP-processed Cu using accelerator-based gamma-ray-induced positron annihilation spectroscopy and neutron diffraction, Mater. Trans. 54 (2013) 1562-1569.

[60] F. Salimyanfard, M.R. Toroghinejad, F. Ashrafizadeh, M. Hoseini, J.A. Szpunar, Investigation of texture and mechanical properties of copper processed by new route of equal channel angular pressing, Mater. Des. 44 (2013) 374-381.

[61] A.P. Zhilyaev, T.G. Langdon, Microhardness and EBSD microstructure mapping in partially-pressed Al and Cu through 90 degrees ECAP die, Mater. Res. 16 (2013) 586-591.

[62] W. Blum, J. Dvořák, P. Král, P. Eisenlohr, V. Sklenička, Effect of grain refinement by ECAP on creep of pure Cu, Mater. Sci. Eng. A590 (2014) 423-432.

[63] P. Zhang, S. Qu, M.X. Yang, G. Yang, S.D. Wu, S.X. Li, Z.F. Zhang, Varying tensile fracture mechanisms of Cu and Cu-Zn alloys with reduced grain size: From necking to shearing instability, Mater. Sci. Eng. A594 (2014) 309-320.

[64] O.F. Higuera-Cobos, J.A. Berrios-Ortiz, J.M. Cabrera, Texture and fatigue behavior of ultrafine grained copper produced by ECAP, Mater. Sci. Eng. A609 (2014) 273-282.

[65] T. Kvackaj, A. Kovacova, R. Kocisko, J. Dutkiewicz, L. Litynska-Dobrzynska, J. Kansy, Relation between microstructural features and mechanical properties in oxygen free high conductivity copper after equal-channel angular pressing, Kovove Mater. 52 (2014) 337-344.

[66] J. Dvořák, P. Král, M. Svoboda, M. Kvapilova, V. Sklenička, Enhanced creep properties of copper and its alloys processed by ECAP, IOP Conf. Series: Mater. Sci. Eng. 63 (2014) 012141.

[67] Y.L. Wang, R. Lapovok, J.T. Wang, Y.S. Qi, Y. Estrin, Thermal behavior of copper processed by ECAP with and without back pressure, Mater. Sci. Eng. A628 (2015) 21-29.

[68] V. Bratov, E.N. Borodin, Comparison of dislocation density based approaches for prediction of defect structure evolution in aluminium and copper processed by ECAP, Mater. Sci. Eng. A631 (2015) 10-17.

[69] S.R. Bahadori, K. Dehghani, Influence of intermediate annealing on the nanostructure and mechanical properties of pure copper processed by equal channel angular pressing and cold rolling, Metall. Mater. Trans. 46A (2015) 2796-2802.

[70] S.R. Bahadori, K. Dehghani, S.A.A. Akbari Mousavi, Comparison of microstructure and mechanical properties of pure copper processed by twist extrusion and equal channel angular pressing, Mater. Lett. 152 (2015) 48-52.

[71] M. Goto, K. Morita, J. Kitamura, M. Baba, S.-Z. Han, J.-H. Ahn, S. Kim, Fatigue-induced damage and crack growth of Cu processed by ECAP, Modern Phys. Lett. B 29 (2015) 1540028.

[72] H. Jiang, Y.T. Zhu, D.P. Butt, I.V. Alexandrov, T.G. Lowe, Microstructural evolution, microhardness and thermal stability of HPT-processed Cu, Mater. Sci. Eng. A290 (2000) 128-138.

[73] T. Hebesberger, H.P. Stüwe, A. Vorhauer, F. Wetscher, R. Pippan, Structure of Cu deformed by high pressure torsion, Acta Mater. 53 (2005) 393-402.

[74] Y.H. Zhao, X.Z. Liao, Y.T. Zhu, Z. Horita, T.G. Langdon, Influence of stacking fault energy on nanostructure formation under high pressure torsion, Mater. Sci. Eng. A410-411 (2005) 188-193.

[75] F. Wetscher, A. Vorhauer, R. Pippan, Strain hardening during high pressure torsion deformation, Mater. Sci. Eng. A410-411 (2005) 213-216.

[76] Z. Horita, T.G. Langdon, Microstructures and microhardness of an aluminum alloy and pure copper after processing by high-pressure torsion, Mater. Sci. Eng. A410-411 (2005) 422-425.

[77] Y.H. Zhao, Y.T. Zhu, X.Z. Liao, Z. Horita, T.G. Langdon, Tailoring stacking fault energy for high ductility and high strength in ultrafine grained Cu and its alloy, Appl. Phys. Lett. 89 (2006) 121906.

[78] E. Schafler, A. Dubravina, B. Mingler, H.P. Karnthaler, M. Zehetbauer, On the microstructure of HPT processed Cu under variation of deformation parameters, Mater. Sci. Forum 503-504 (2006) 51-56.

[79] V.D. Sitdikov, R.G. Chembarisova, I.V. Alexandrov, Analysis of the deformation behaviour of Cu processed by high pressure torsion, Solid State Phenom. 114 (2006) 101-106.

[80] T. Ungár, L. Balogh, Y.T. Zhu, Z. Horita, C. Xu, T.G. Langdon, Using X-ray microdiffraction to determine grain sizes at selected positions in disks processed by high-pressure torsion, Mater. Sci. Eng. A444 (2007) 153-156.

[81] E. Schafler, M.B. Kerber, Microstructural investigation of the annealing behaviour of high-pressure torsion (HPT) deformed copper, Mater. Sci. Eng. A462 (2007) 139-143.

[82] J. Čížek, I. Procházka, M. Cieslar, R. Kužel, Z. Matěj, V. Cherkaska, R. K. Islamgaliev, O. Kulyasova, Influence of ceramic nanoparticles on grain growth in ultrafine grained copper prepared by high pressure torsion, Phys. Stat. Sol. C 4 (2007) 3587-3590.

[83] L. Balogh, T. Ungár, Y. Zhao, Y.T. Zhu, Z. Horita, C. Xu, T.G. Langdon, Influence of stacking-fault energy on microstructural characteristics of ultrafine-grain copper and copper–zinc alloys, Acta Mater. 56 (2008) 809-820.

[84] Y.H. Zhao, Z. Horita, T.G. Langdon, Y.T. Zhu, Evolution of defect structures during cold rolling of ultrafine-grained Cu and Cu-Zn alloys: Influence of stacking fault energy, Mater. Sci. Eng. A474 (2008) 342-347.

[85] K. Edalati, T. Fujioka, Z. Horita, Microstructure and mechanical properties of pure Cu processed by high-pressure torsion, Mater. Sci. Eng. A 497 (2008) 168-173.

[86] B.J. Bonarski, B. Mikulowski, E. Schafler, C. Holzleithner, M.J. Zehetbauer, Crystallographic textures of single and polycrystalline pure Mg and Cu subjected to HPT deformation, Arch. Metall. Mater. 53 (2008) 117-123.

[87] Z.L. Xie, X.L. Wu, J.J. Xie, Y.S. Hong, Microstructures and compression properties of copper specimens deformed by high-pressure torsion, Acta Metall. Sinica 44 (2008) 803-809.

[88] A.R. Kilmametov, G. Vaughan, A.R. Yavari, A. LeMoulec, W.J. Botta, R.Z. Valiev, Microstructure evolution in copper under severe plastic deformation detected by in situ X-ray diffraction using monochromatic synchrotron light, Mater. Sci. Eng. A503 (2009) 10-13.

[89] K. Edalati, Y. Ito, K. Suehiro, Z. Horita, Softening of high purity aluminum and copper processed by high pressure torsion, Intl. J. Mater. Res. 100 (2009) 1668-1673.

[90] X.H. An, S.D.Wu, Z.F. Zhang, R.B. Figueiredo, N. Gao and T.G. Langdon, Evolution of microstructural homogeneity in copper processed by high-pressure torsion, Scripta Mater. 63 (2010) 560-563.

[91] G. Khatibi, J. Horky, B. Weiss, M.J. Zehetbauer, High cycle fatigue behaviour of copper deformed by high pressure torsion, Intl. J. Fatigue 32 (2010) 269-278.

[92] Z.L. Xie, X.L. Wu, J.J. Xie, Y.S. Hong, Analysis of the thermal stability of copper specimens deformed by high-pressure torsion, Acta Metall. Sinica 46 (2010) 458-465.

[93] J. Čížek, M. Janeček, O. Srba, R. Kužel, Z. Barnovská, I. Procházka, S. Dobatkin, Evolution of defects in copper deformed by high-pressure torsion, Acta Mater. 59 (2011) 2322-2329.

[94] Y. Song, E.Y. Yoon, D.J. Lee, J.H. Lee, H.S. Kim, Mechanical properties of copper after compression stage of high-pressure torsion, Mater. Sci. Eng. A528 (2011) 4840-4844.

[95] J. Gubicza, S.V. Dobatkin, E. Khosravi, A.A. Kuznetsov, J.L. Labar, Microstructural stability of Cu processed by different routes of severe plastic deformation, Mater. Sci. Eng. A528 (2011) 1828-1832.

[96] K. Edalati, R. Miresmaeili, Z. Horita, H. Kanayama, R. Pippan, Significance of temperature increase in processing by high-pressure torsion, Mater. Sci. Eng. A528 (2011) 7301-7305.

[97] X.H. An, Q.Y. Lin, S.D. Wu, Z.F. Zhang, R.B. Figueiredo, N. Gao, T.G. Langdon, Significance of stacking fault energy on microstructural evolution in Cu and Cu-Al alloys processed by high-pressure torsion, Phil. Mag. 91 (2011) 3307-3326.

[98] K.J. Al-Fadhalah, S.N. Alhajeri, A.I. Almazrouee, T.G. Langdon, Microstructure and microtexture in pure copper processed by high-pressure torsion, J. Mater. Sci. 48 (2013) 4563-4572.

[99] M. Wegner, J. Leuthold, M. Peterlechner, D. Setman, M. Zehetbauer, R. Pippan, S.V. Divinski, G. Wilde, Percolating porosity in ultrafine grained copper processed by high pressure torsion, J. Appl. Phys. 114 (2013) 183509.

[100] H.M. Wen, R.K. Islamgaliev, K.M. Nesterov, R.Z. Valiev, E.J. Lavernia, Dynamic balance between grain refinement and grain growth during high-pressure torsion of Cu powders, Phil. Mag. Lett. 93 (2013) 481-489.

[101] P. Jenei, J. Gubicza, E.Y. Yoon, H.S. Kim, J.L. Labar, High temperature thermal stability of pure copper and copper-carbon nanotube composites consolidated by high pressure torsion, Composites A (2013) 71-79.

[102] J. Horky, G. Khatibi, D. Setman, B. Weiss, M.J. Zehetbauer, Effect of microstructural stability on fatigue crack growth behaviour of nanostructured Cu, Mechanics Mater. 67 (2013) 38-45.

[103] B. Oberdorfer, D. Setman, E.-M. Steyskal, A. Hohenwarter, W. Sprengel, M. Zehetbauer, R. Pippan, R. Würschum, Grain boundary excess volume and defect annealing of copper after high-pressure torsion, Acta Mater. 68 (2014) 189-195.

[104] O. Renk, A. Hohenwarter, S. Wurster and R. Pippan, Direct evidence for grain boundary motion as the dominant restoration mechanism in the steady-state regime of extremely cold-rolled copper, Acta Mater. 77 (2014) 401-410.

[105] E.Y. Yoon, D.J. Lee, L.J. Park, S. Lee, M.I. Abd El Aal, H.S. Kim, Effect of post-annealing on grain boundary of nano-crystalline Cu processed by powder high-pressure torsion, Metall. Mater. Trans. 45A (2014) 4748-4752.

[106] M. Jahedi, M.H. Paydar, S. Zheng, I.J. Beyerlein, M. Knezevic, Texture evolution and enhanced grain refinement under high-pressure-double-torsion, Mater. Sci. Eng. A611 (2014) 29-36.

[107] A.P. Zhilyaev, I. Shakhova, A. Belyakov, R. Kaibyshev, T.G. Langdon, Effect of annealing on wear resistance and electroconductivity of copper processed by high-pressure torsion, J. Mater. Sci. 49 (2014) 2270-2278.

[108] A.P. Zhilyaev and T.G. Langdon, Long-term self-annealing of copper and aluminium processed by high-pressure torsion, J. Mater. Sci. 49 (2014) 6529-6535.

[109] A.P. Zhilyaev, S.N. Sergeev and T.G. Langdon, Electron backscatter diffraction (EBSD) microstructure evolution in HPT copper annealed at a low temperature, J. Mater. Res. Tech. 3 (2014) 338-343.

[110] A. Hohenwarter, Incremental high pressure torsion as a novel severe plastic deformation process: Processing features and application to copper, Mater. Sci. Eng. A626 (2015) 80-85.

[111] A.I. Almazrouee, K.J. Al-Fadhalah, S.N. Alhajeri, T.G. Langdon, Microstructure and microhardness of OFHC copper processed by high-pressure torsion, Mater. Sci. Eng. A641 (2015) 21-28.

[112] J. Xu, J. Li, C.T. Wang, D. Shan, B. Guo, T.G. Langdon, Evidence for an early softening behaviour in pure copper processed by high-pressure torsion, J. Mater. Sci. (2016) DOI: 10.1007/s10853-015-9499-6.

[113] J. Li, J. Xu, C.T. Wang, D. Shan, B. Guo, T.G. Langdon, Microstructural evolution and micro-compression in high-purity copper processed by high-pressure torsion, Adv, Eng. Mater. (2016) DOI: 10.002/adem.201500488.

[114] A.P. Zhilyaev, S. Swaminathan, A.A. Gimazov, T.R. McNelley, T.G. Langdon, An evaluation of microstructure and microhardness in copper subjected to ultra-high strains, J. Mater. Sci. 43 (2008) 7451-7456.

[115] A.P. Zhilyaev, A.A. Gimazov, T.G. Langdon, Recent developments in modelling of microhardness saturation during SPD processing of metals and alloys, J. Mater. Sci. 48 (2013) 4461-4466.

[116] J. Schamp, B. Verlinden, J. Van Humbeeck, Recrystallisation at ambient temperature of heavily deformed ETP copper wire, Scripta Mater. 34 (1996) 1667-1672.

[117] T. Konkova, S. Mironov, A. Korznikov, S.L. Semiatin, On the room-temperature annealing of cryogenically rolled copper, Mater. Sci. Eng. A528 (2011) 7432-7443.

[118] O.V. Mishin, A. Godfrey, Microstructure of ECAE-processed copper after long-term room-temperature storage, Metall. Mater. Trans. A 39A (2008) 2923-2930.

[119] G. Wang, S.D. Wu, L. Zuo, C. Esling, Z.G. Wang, G.Y. Li, Microstructure, texture, grain boundaries in recrystallization regions in pure Cu ECAE samples, Mater. Sci. Eng. A346 (2003) 83-90.

[120] J. Gubicza, N.Q. Chinh, J.L. Lábár, Z. Hegedüs, P. Szommer, G. Tichy, T.G. Langdon, Delayed microstructural recovery in silver processed by equal-channel angular pressing, J. Mater. Sci. 43 (2008) 5672-5676.

[121] J. Gubicza, N.Q. Chinh, J.L. Lábár, Z. Hegedüs, T.G. Langdon, Principles of self-annealing in silver processed by equal-channel angular pressing: The significance of a very low stacking fault energy, Mater. Sci. Eng. A527 (2010) 752-760.

[122] M. Kawasaki, Different models of hardness evolution in ultrafine-grained materials processed by high-pressure torsion, J. Mater. Sci. 49 (2014) 18-34.

[123] I. Balasundar, K.R. Ravi, T. Raghu, Strain softening in oxygen free high conductivity (OFHC) copper subjected to repetitive upsetting-extrusion (RUE) process, Mater. Sci. Eng. A583 (2013) 114-122.

[124] R.B. Figueiredo, P.R. Cetlin, T.G. Langdon, Using finite element modeling to examine the flow processes in quasi-constrained high-pressure torsion Mater. Sci. Eng. A 528 (2011) 8198-8204.

[125] R.B. Figueiredo, P.H.R. Pereira, M.T.P. Aguilar, P.R. Cetlin, T.G. Langdon, Using finite element modeling to examine the temperature distribution in quasi-constrained high-pressure torsion, Acta Mater. 60 (2012) 3190-3198.

[126] H.M. Rietveld, A profile refinement method for nuclear and magnetic structures, Journal of Applied Crystallography 2 (1969) 65-71.

[127] C. Xu, Z. Horita, T.G. Langdon, Microstructural evolution in pure aluminum in the early stages of processing by high-pressure torsion, Mater. Trans. 51 (2010) 2-7.

[128] D.P. Field, L.T. Bradford, M.M. Nowell, T.M. Lillo, The role of annealing twins during recrystallization of Cu, Acta Mater. 55 (2007) 4233-4241.

[129] G.K. Williamson, R.E. Smallman, Dislocation densities in some annealed and cold-worked metals from measurements on the X-ray Debye-Scherrer spectrum, Philos. Mag. 1 (1956) 34-46.

[130] R.E. Smallman, K.H. Westmacott, Stacking faults in face-centred cubic metals and alloys, Philos. Mag. 2 (1957) 669-683.

[131] Y.H. Zhao, X.Z. Liao, Z. Jin, R.Z. Valiev, Y.T. Zhu, Microstructures and mechanical properties of ultrafine grained 7075 Al alloy processed by ECAP and their evolutions during annealing, Acta Mater. 52 (2004) 4589-4599.

[132] K. Edalati, J.M. Cubero-Sesin, A. Alhamidi, I.F. Mohamed, Z. Horita, Influence of severe plastic deformation at cryogenic temperature on grain refinement and softening of pure metals: Investigation using high-pressure torsion, Mater. Sci. Eng. A 613 (2014) 103-110.

[133] R.Z. Valiev, Yu.V. Ivanisenko, E.F. Rauch, B. Baudelet, Structure and deformaton behaviour of Armco iron subjected to severe plastic deformation, Acta Mater. 44 (1996) 4705-4712.

[134] F. Wetscher, A. Vorhauer, R. Stock, R. Pippan, Structural refinement of low alloyed steels during severe plastic deformation, Mater. Sci. Eng. A 387-389 (2004) 809-816.

[135] F. Wetscher, R. Pippan, S. Sturm, F. Kauffmann, C. Scheu, G. Dehm, TEM investigations of the structural evolution in a pearlitic steel deformed by high-pressure torsion, Metall. Mater. Trans. A 37 (2006) 1963-1968.

[136] M. Kawasaki, B. Ahn, T.G. Langdon, Microstructural evolution in a two-phase alloy processed by high-pressure torsion, Acta Mater 58 (2010) 919-930.

[137] M. Kawasaki, B. Ahn and T.G. Langdon, Significance of strain reversals in a two-phase alloy processed by high-pressure torsion, Mater Sci Eng A 527 (2010) 7008-7016.

[138] A. Vorhauer, R. Pippan, On the homogeneity of deformation by high pressure torsion, Scripta Mater. 51 (2004) 921-925.

[139] C. Xu, Z. Horita, T.G. Langdon, The evolution of homogeneity in processing by high-pressure torsion, Acta Mater. 55 (2007) 203-212.

[140] S. Erbel, Mechanical properties and structure of extremely strain-hardened copper, Metals Tech. 6 (1979) 482-486.

[141] I. Sanders, J. Nutting, Deformation of metals to high strains using combination of torsion and compression, Metal Sci. 18 (1984) 571-575.

[142] M. Kawasaki, Z. Horita, T.G. Langdon, Microstructural evolution in high purity aluminum processed by ECAP, Mater. Sci. Eng. A 524 (2009) 143-150.

[143] B. Oberdorfer, B. Lorenzoni, K. Unger, W. Sprengel, M. Zehetbauer, R. Pippan and R. Würschum, Absolute concentration of free volume-type defects in ultrafine-grained Fe prepared by high-pressure torsion, Scripta Mater. 63 (2010) 452-455.

[144] D. Setman, M. Kerber, H. Bahmanpour, J. Horky, R.O. Scattergood, C.C. Koch, M.J. Zehetbauer, Nature and density of lattice defects in ball milled nanostructured copper, Mech. Mater. 67 (2013) 59-64.

[145] X. Sauvage, G. Wilde, S. Divinski, Z. Horita, R.Z. Valiev, Grain boundaries in ultrafine grained materials processed by severe plastic deformation and related phenomena, Mater. Sci. Eng. A 540 (2012) 1-12.

Figure captions

Fig. 1 Hardness plotted against the position on the disc at 48 h after HPT processing.

Fig. 2 Microstructures of discs at 48 h after HPT processing for 1/2 turn (upper) and 10 turns (lower): images are shown for different positions on the discs.

Fig. 3 Hardness measurements recorded along disc diameters at 48 h after HPT and after post-HPT RT storage for different times up to 6 weeks for samples processed through (a) 1/2, (b) 1, (c) 5 and (d) 10 turns.

Fig. 4 Microstructural evolution during post-HPT RT storage for a disc processed through 1/2 turn.

Fig. 5 The fractional numbers of grain boundary misorientation angles for different RT storage times for the disc processed through 1/2 turn measured at 3.5 mm from the disc centre.

Fig.6 Grain boundary character distributions for the disc processed through 1/2 turn at 3.5 mm from the disc centre showing the effect of different RT storage times.

Fig. 7 Variation of the measured microstrains and the dislocation densities determined from XRD analysis with the numbers of turns in HPT processing during RT storage for (a) 1 h, (b) 1 week and (c) 4 weeks.

Fig. 8 Estimated crystallite sizes plotted against the time of RT storage for discs processed through (a) 1/2 and (b) 10 turns.

Fig. 9 Values of the Vickers microhardness recorded at 48 h after HPT processing plotted as a function of the equivalent strain for discs processed through different numbers of turns.

Table caption

Table 1 Chemical composition of OFHC copper (wt.%)

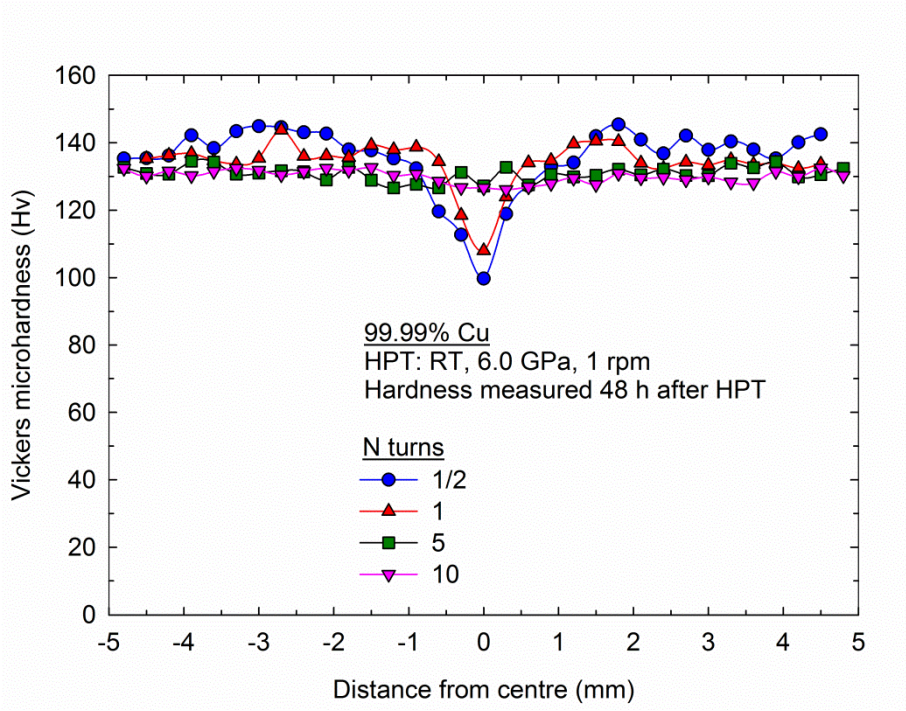

Fig. 1 Hardness plotted against the position on the disc at 48 h after HPT processing.

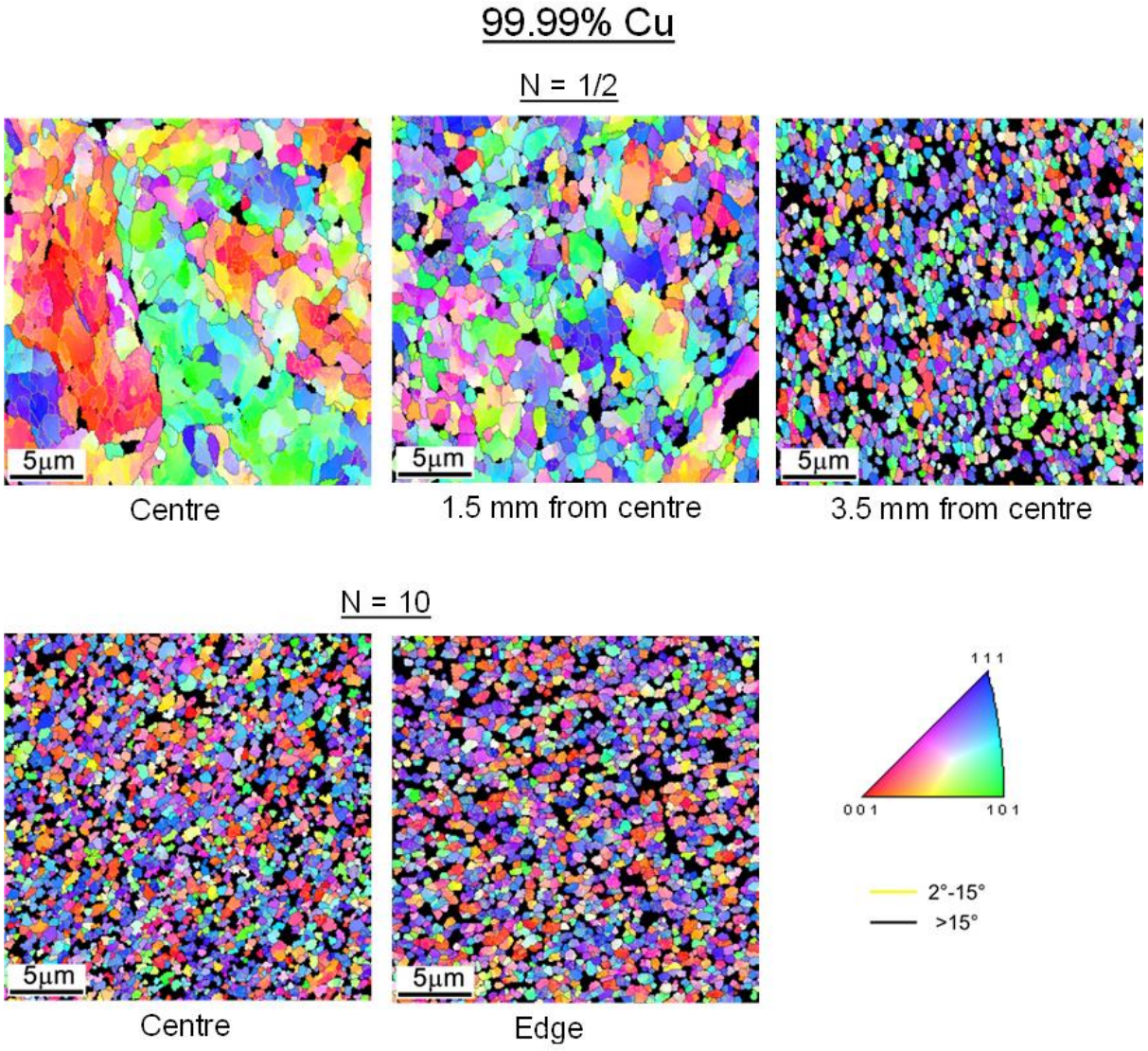

Fig. 2 Microstructures of discs at 48 h after HPT processing for 1/2 turn (upper) and 10 turns (lower): images are shown for different positions on the discs.

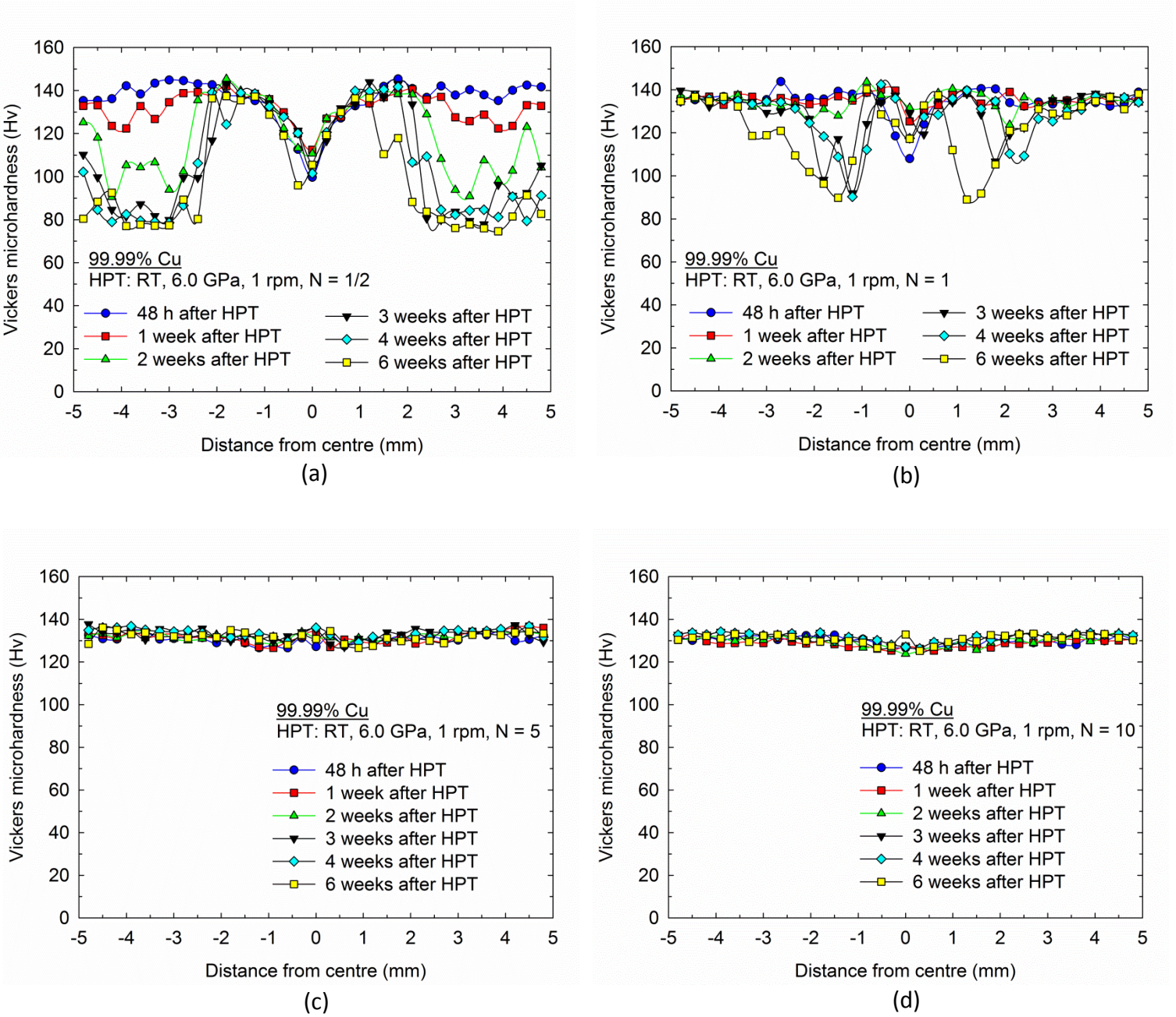

Fig. 3 Hardness measurements recorded along disc diameters at 48 h after HPT and after post-HPT RT storage for different times up to 6 weeks for samples processed through (a) 1/2, (b) 1, (c) 5 and (d) 10 turns.

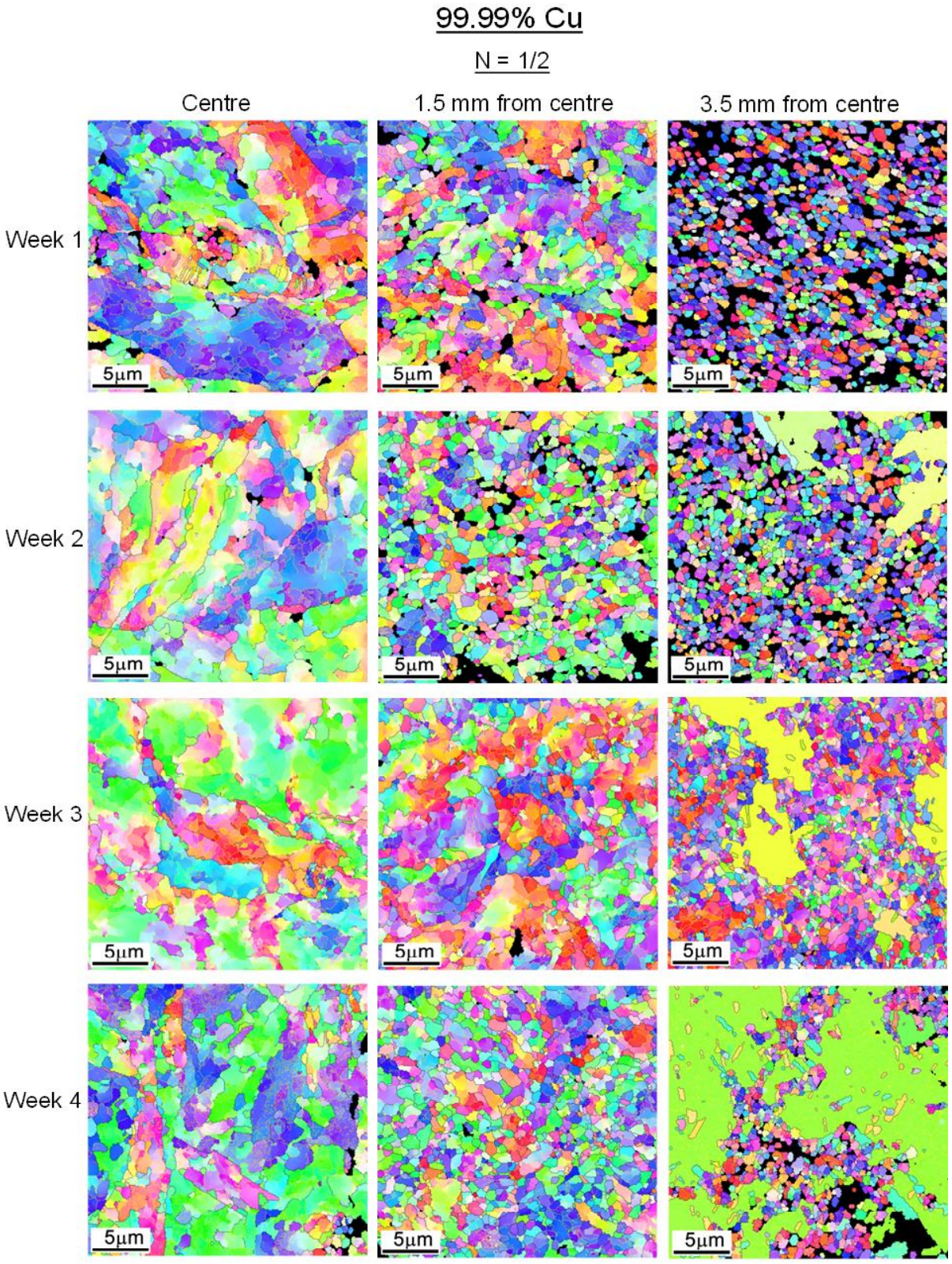

Fig. 4 Microstructural evolution during post-HPT RT storage for a disc processed through 1/2 turn.

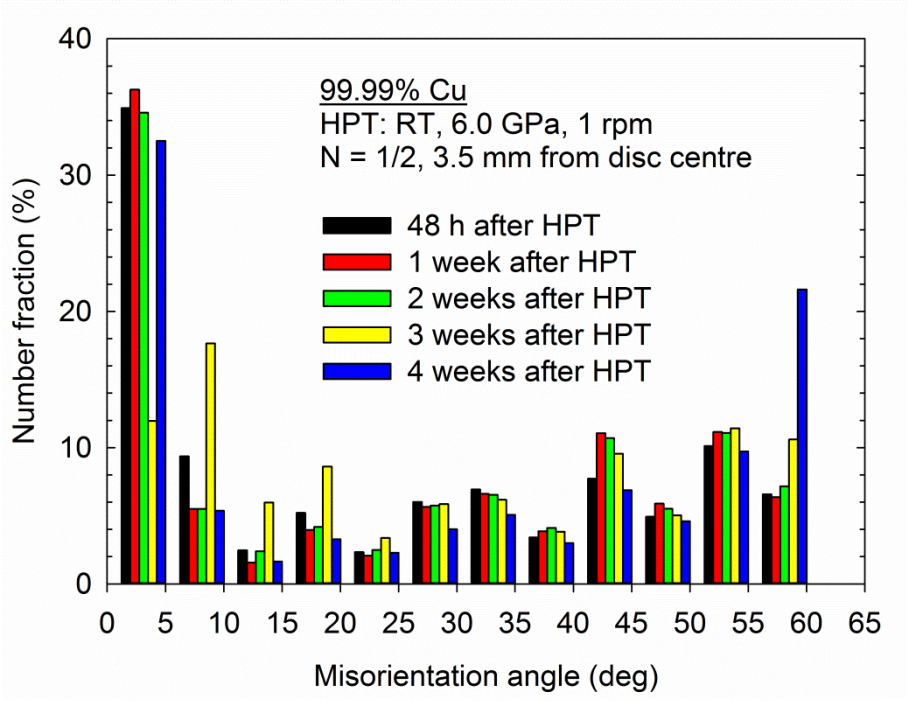

Fig. 5 The fractional numbers of grain boundary misorientation angles for different RT storage times for the disc processed through 1/2 turn measured at 3.5 mm from the disc centre.

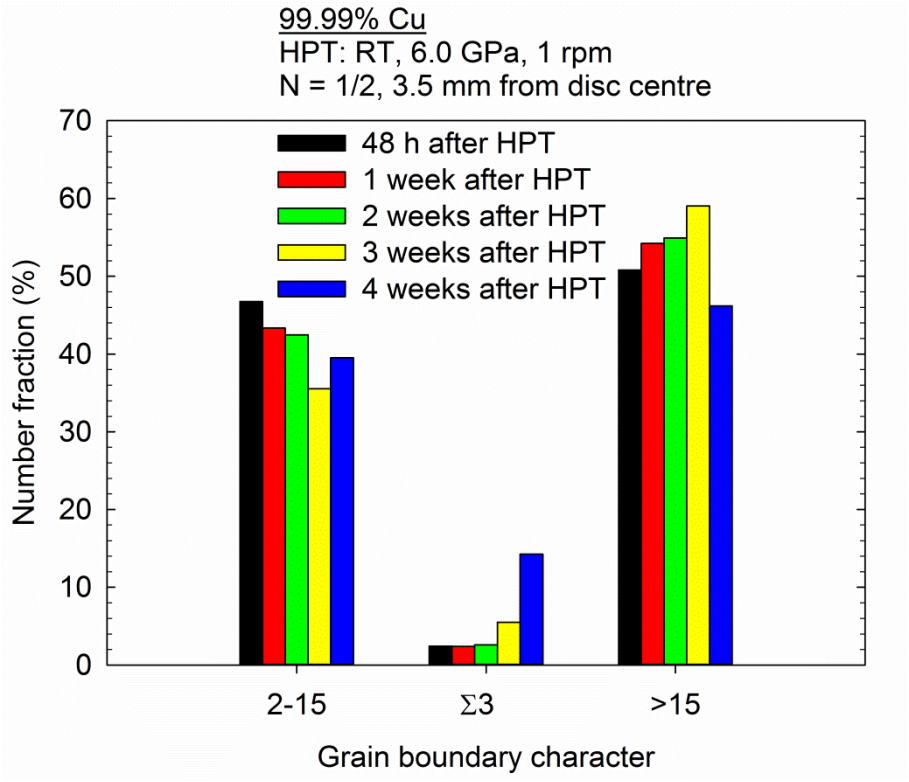

Fig.6 Grain boundary character distributions for the disc processed through 1/2 turn at 3.5 mm from the disc centre showing the effect of different RT storage times.

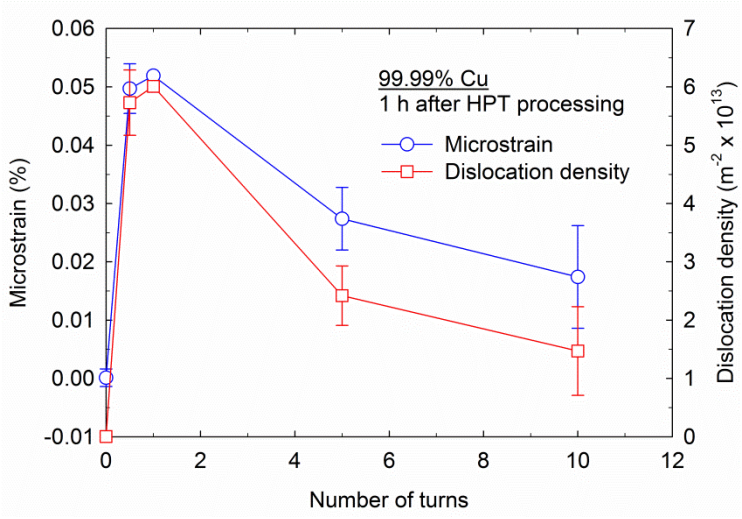

(a)

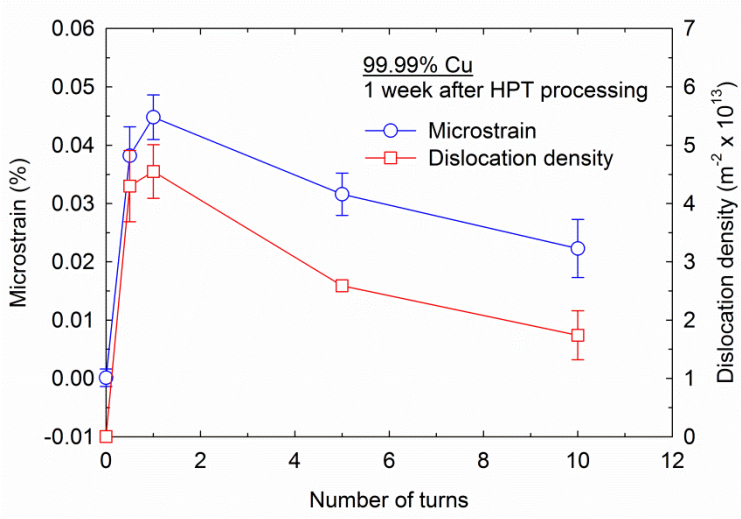

(b)

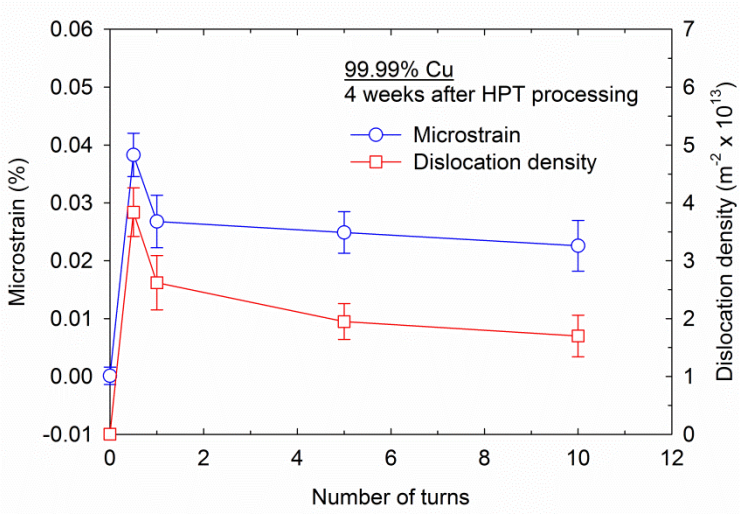

(c)

Fig. 7 Variation of the measured microstrains and the dislocation densities determined from XRD analysis with the numbers of turns in HPT processing during RT storage for (a) 1 h, (b) 1 week and (c) 4 weeks.

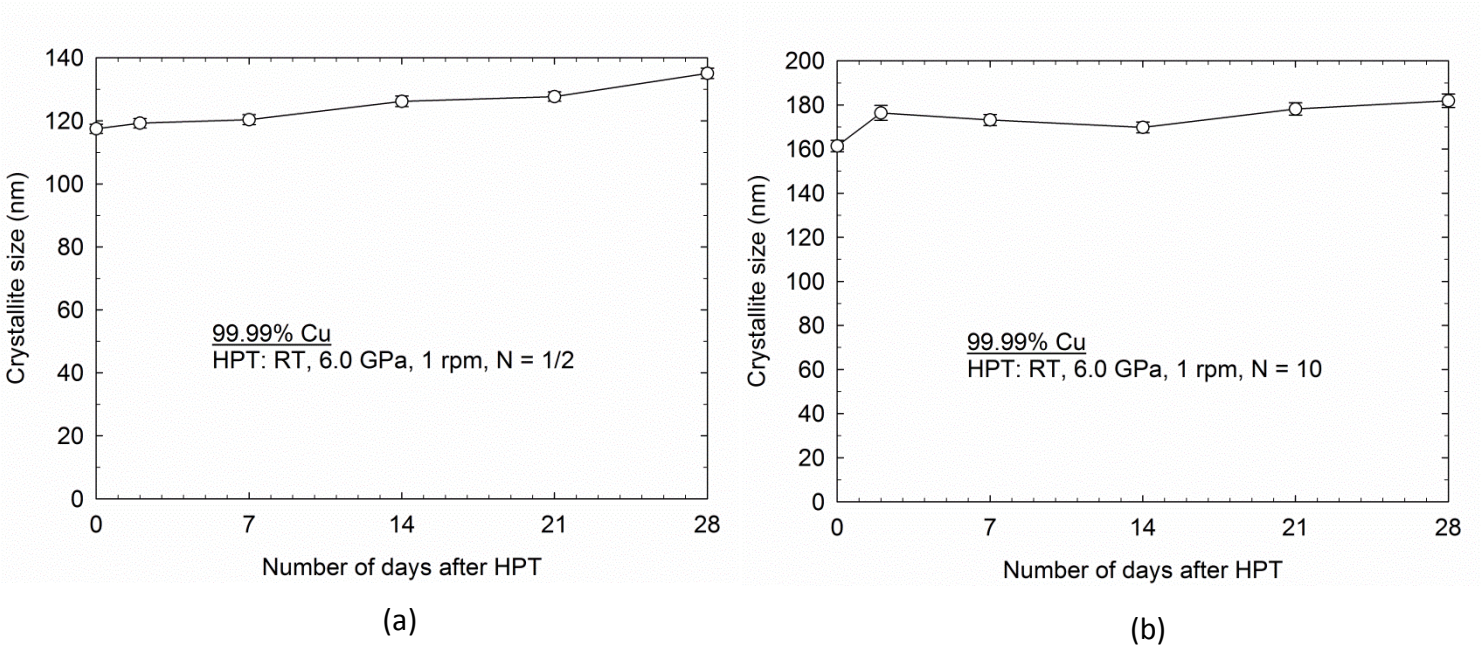

Fig. 8 Estimated crystallite sizes plotted against the time of RT storage for discs processed through (a) 1/2 and (b) 10 turns.

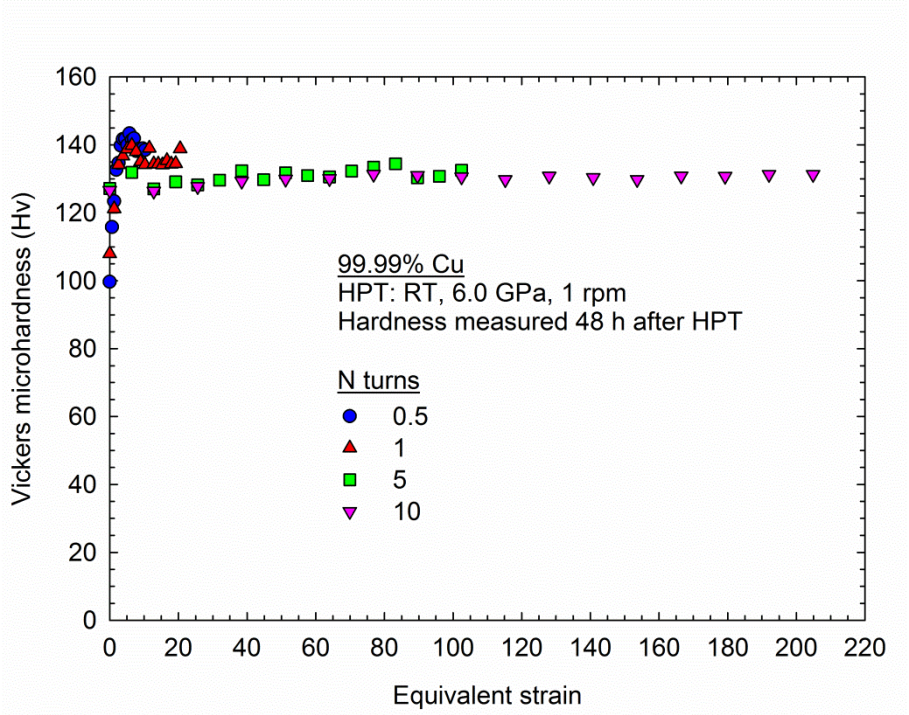

Fig. 9 Values of the Vickers microhardness recorded at 48 h after HPT processing plotted as a function of the equivalent strain for discs processed through different numbers of turns.

Table1 Chemical composition of OFHC copper (wt.%)

Sample/Element	Ag	As	Bi	Cd	Fe	Mn	I	O	P	Pb	S	Sb	Se	Sn	Te	Zn	Cu
OFHC Cu	0.0025	0.0005	0.0001	0.0001	0.001	0.00005	0.001	0.0005	0.0003	0.0005	0.0015	0.0004	0.0003	0.0002	0.0002	0.0001	99.99*

* Minimum guaranteed percentage of Cu